

Ion-Bernstein-Wave Heating in the JIPPT-II-U Tokamak Plasma

M. Ono,^(a) T. Watari, R. Ando, J. Fujita, Y. Hirokura, K. Ida,^(a) E. Kako, K. Kawahata, Y. Kawasumi, K. Matsuoka, A. Nishizawa, N. Noda, I. Ogawa, K. Ohkubo, M. Okamoto, K. Sato, S. Tanahashi, Y. Taniguchi, T. Tetsuka, K. Toi, and K. Yamazaki

Institute of Plasma Physics, Nagoya University, Nagoya 464, Japan

(Received 27 February 1985)

Ion-Bernstein-wave heating is investigated in the JIPPT-II-U tokamak plasma, $\bar{n}_e \approx 1.5 \times 10^{13} \text{ cm}^{-3}$, $T_{e0} \approx 700 \text{ eV}$, and $T_{i0} \approx 300 \text{ eV}$ for $P_{rf} \leq 100 \text{ kW}$. When the $\frac{3}{2}\Omega_H$ layer is placed near the plasma minor axis, the bulk-hydrogen-ion temperature shows a significant rise, $\Delta T_{i\perp} \leq 700 \text{ eV}$ and $\Delta T_{i\parallel} \leq 300 \text{ eV}$. The ion-heating dependence on the magnetic field and rf power suggests a presence of a direct bulk-hydrogen heating mechanism at $\omega \approx \frac{3}{2}\Omega_H$.

PACS numbers: 52.50.Gj, 52.55.Fa

Ion-Bernstein-wave heating is an ion-cyclotron-resonance-frequency heating concept that utilizes directly launched ion-Bernstein waves to carry the rf power deep into the reactor plasma core. Ray-tracing calculations predict that the ion-Bernstein waves (IBW) have excellent accessibility to the hot, dense core of reactorlike plasmas for a wide range of launched parallel index of refraction, $n_{\parallel} \equiv ck_{\parallel}/\omega$.¹ Because its short-wavelength nature makes the perpendicular-wave phase velocity comparable to the ion thermal velocity ($\omega/k_{\perp} \approx V_{ti}$), IBW is expected to heat bulk ions even at relatively high ion cyclotron harmonics of fusion ions. In the recent ACT-I experiment, an excellent bulk-ion heating with a quality factor, commonly defined as a product of the peak ion-temperature rise and the line-averaged density normalized by the loaded rf power, of $\Delta T_{i\perp} \bar{n}_e / P_{rf} \approx 10 \text{ eV} \times 10^{10} \text{ cm}^{-3}/\text{W}$ has been observed for the density range of $n_e \approx 10^{10} - 10^{11} \text{ cm}^{-3}$.² The present JIPPT-II-U experiment represents the first experimental attempt to test this heating concept in a realistic, sheared tokamak plasma with a significant scaling up of parameters from the ACT-I experiment. The JIPPT-II-U plasma has a major radius (R_0) of 91 cm and a minor radius (r_0) of 23 cm which was recently increased from 15 cm.³

Figure 1(a) shows a schematic of the IBW antenna, which is a B_{θ} -loop antenna (a Nagoya type-III antenna⁴) with poloidal Faraday shield to simulate a single- E_z -waveguide antenna. The coupling to the fast wave should be minimal for this antenna.⁵ In ACT-I, this type of loop antenna was observed to launch a radially inward-propagating IBW wave packet with good loading characteristics.^{5,6} In the present experiment, a 40-MHz transmitter has been used which is suitable for the second-harmonic IBW launching⁷ in a hydrogen plasma at 1.8-T toroidal field B_0 which is given at $R = 91 \text{ cm}$. Typically 80% of the transmitter power is coupled to the plasma. The rf power is defined here to be that of the power coupled to the plasma.

The wave-power absorption can be provided by the

third ion-cyclotron harmonic of deuteriumlike ions. In this experiment, the deuteriumlike ions are introduced by addition of ^4He to the hydrogen gas, using a premixed He-H gas of known concentration. The helium concentration quoted in this paper is that of the premixed value, since the actual ion concentration in the center of the plasma is not known. One should note that if the low- z impurity level is sufficient, those fully stripped impurity ions ($\text{C}^{+6}, \text{O}^{+8}$) can also provide the absorption layer. Although the experimental observation as we shall describe here does not quite agree with this linear-theory picture, it may be helpful to discuss what is expected from the linear theory. To calculate for the power deposition profiles, we used the tokamak ray-tracing code,¹ which contains the well-known linear-absorption processes such as the ion-cyclotron-harmonic damping and electron Landau damping. In Fig. 1(b), we show the calculated wave-power deposition profiles for our typical plasma parameters for the optimum field, $B_0 = 1.8 \text{ T}$, and for the off-axis case, $B_0 = 1.89 \text{ T}$. As can be seen in the figure, at the optimum field ($B_0 = 1.8 \text{ T}$), the resonance absorption-layer position is very close to the plasma-axis position ($R \approx 93 \text{ cm}$). In the inset, the ray trajectories are shown where the rays are released from various antenna poloidal positions to reflect the finite size of the antenna structure. One can see that the rays follow roughly horizontal paths and show slight focusing behavior toward the minor axis. The wave power-deposition profile for the on-axis heating case is much more peaked than the off-axis case because of the smaller heating volume. Therefore, under normal confinement conditions, we expect the heating to be strongly optimized near $B_0 = 1.8 \text{ T}$.

Representative traces of the Ohmic discharge used in the experiment are shown in Fig. 1(b); $I_p \approx 110 \text{ kA}$ [$q(\text{edge}) \approx 4.0$], $\bar{n}_e \approx 1.5 \times 10^{13} \text{ cm}^{-3}$, $T_{e0} \approx 700 \text{ eV}$, and $T_{i0} \approx 300 \text{ eV}$, where I_p is the Ohmic current and q is the safety factor. The toroidal field, $B_0 \approx 1.8 \text{ T}$, remains essentially flat during the heating. The plasma density rises during rf as can be seen in Fig. 1(b).

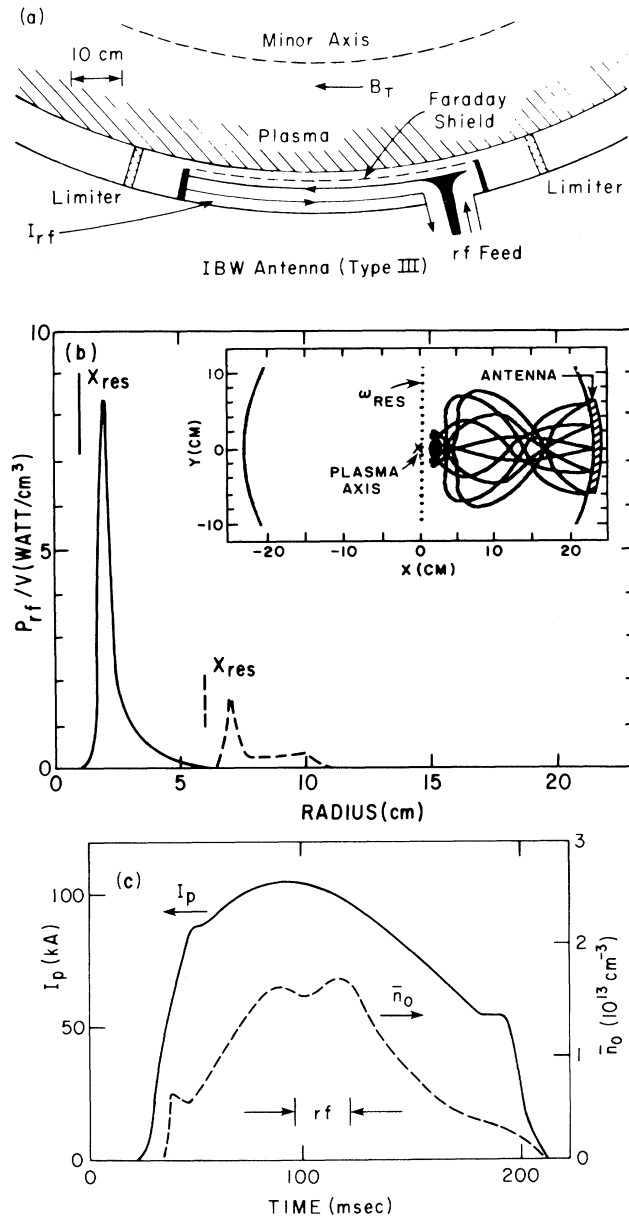


FIG. 1. (a) Schematic of IBW B_θ -loop antenna. (b) Power deposition profiles of IBW for $B_0 = 1.8$ T (solid curve) and for $B_0 = 1.89$ T (dashed curve). $T_{i0} = 300$ eV, $T_{e0} = 700$ eV, $\bar{n}_e = 1.5 \times 10^{13} \text{ cm}^{-3}$, 10% H_e , $f = 40$ MHz, and $P_{rf} = 60$ kW. Inset: Rays with $n_{||} = \pm 3$ released from each poloidal position for $B_0 = 1.8$ T case. (c) Typical Ohmic heating current and line-averaged plasma-density time evolutions.

In Fig. 2, we show typical ion-heating data obtained in a hydrogen discharge with ~ 60 kW of the loaded rf power [Fig. 2(a), inset]. The hydrogen-ion temperature evolution monitored by a perpendicular charge-exchange analyzer is shown as open circles in Fig.

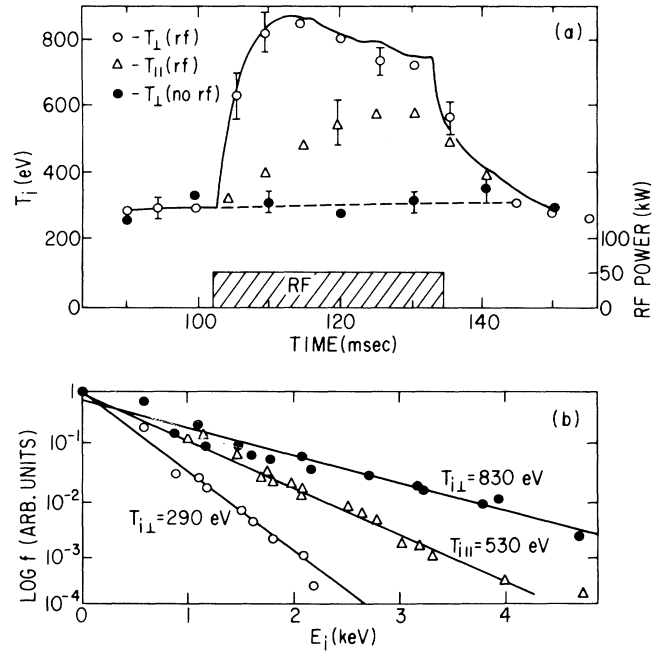


FIG. 2. (a) Ion-temperature time evolution with and without rf. Inset: rf power (loaded). Solid curve: Simulation with the assumption of direct hydrogen heating. (b) Charge-exchange raw signal before and during rf. $B_0 = 1.8$ T, $I_p \approx 110$ kA, $\bar{n}_0 \approx 1.5 \times 10^{13} \text{ cm}^{-3}$, and $f = 40$ MHz.

2(a). The corresponding data without rf are shown as solid circles. The application of rf increases the perpendicular hydrogen-ion temperature from 300 to 800 eV in 5–10 msec. The corresponding charge-exchange raw signal obtained from averaging approximately twenty shots is shown in Fig. 2(b). The velocity distribution appears to be Maxwellian with no significant tail being observed.

To make sure the heated hydrogen ions are completely thermalized as suggested from the linear-heating model, we have moved the charge-exchange analyzer to a tangential port to measure $T_{i||}$. The $T_{i||}$ charge-exchange data taken in a similar plasma discharge with comparable rf power level are shown with open triangles in Fig. 2(a). The corresponding energy distributions are shown in Fig. 2(b). We observe a significant temperature differential between \perp and \parallel hydrogen-ion temperatures, which suggests the presence of a direct hydrogen-ion heating process.

The observed ion heating depends strongly on the magnetic field, as shown by Fig. 3(a), where the perpendicular ion-heating quality factor is plotted as a function of magnetic field with the use of data in the 60–80-kW power range. The ion-heating quality factor peaks near $B_0 = 1.8$ T, corresponding to the $\frac{3}{2} \Omega_H$ layer near the center of the plasma ($R \approx 93$ cm). We note that at this field level, the hydrogen harmonic reso-

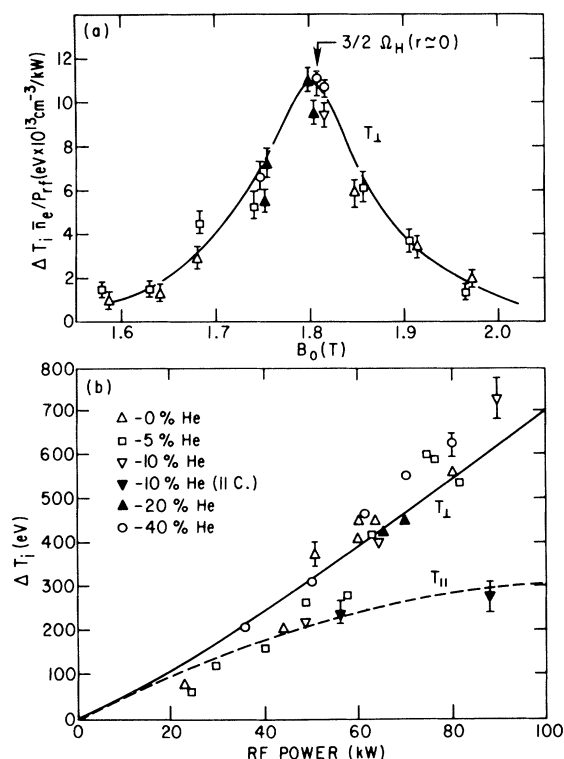


FIG. 3. (a) Ion-heating quality factor, $\Delta T_{i\perp} \bar{n}_e / P_{rf} (\text{eV} \times 10^{13} \text{ cm}^{-3} / \text{kW})$, as a function of toroidal magnetic field, $B_0 (R = 91 \text{ cm})$. He concentrations as labeled. $F = 40 \text{ MHz}$ and $P_{rf}(\text{loaded}) = 60\text{--}80 \text{ kW}$. Solid curve: Simulation value with the assumption of $\Delta r(\text{power deposition}) \approx 4 \text{ cm}$ at $\frac{3}{2} \Omega_H$ layer. (b) $\Delta T_{i\perp}$ and $\Delta T_{i\parallel}$ vs rf power for various He-H gas-mixture concentrations (as labeled). $F = 40 \text{ MHz}$ and $B_0 = 1.8 \text{ T}$. Solid and dashed curves are simulation values for $\Delta T_{i\perp}$ and $\Delta T_{i\parallel}$, respectively.

nance layers, Ω_H and $2\Omega_H$, are completely outside of the plasma, and therefore the usual resonant acceleration of hydrogen ions can be ruled out. An addition of helium ions that can provide $3\Omega_{He}$ resonance absorption at the same location has not produced significant changes in the ion heating as shown in Fig. 3(a). The charge-exchange data, of course, are not affected by the minority ions such as helium and impurities, since they are multiply ionized. The impurity levels are observed to vary little with the magnetic field, showing no correlation with the observed ion heating.

In Fig. 3(b), we show the measured ion-temperature increase as a function of the rf power for various He minority concentrations. The perpendicular ion temperature appears to go up nearly linearly with the rf power. The parallel ion temperature, on the other hand, shows a very nonlinear rise which appears to saturate at high power range.

In order to compare the observed heating result with theory, we have performed a series of model ion-

power-balance calculations using tokamak transport codes. First, by using the tokamak transport code BALDUR⁸ to understand the temporal evolution of the observed ion temperature, we find that the $T_{i\perp}$ rise time matches well with the experimental value if one assumes a direct power description into the hydrogen ions, which is shown as a solid line in Fig. 2(a). If an indirect heating through collisions is assumed, the rise time is slower similar to the $T_{i\parallel}$ rise time. Second, the magnetic field dependence of $T_{i\perp}$ can be reproduced if the rays are assumed to be absorbed at the $\frac{3}{2} \Omega_H$ layer by the \perp component with an effective radial absorption spread of $\sim 4 \text{ cm}$. This result is shown by a solid curve in Fig. 3(a). Finally, in Fig. 3(b), we also show the calculated $\Delta T_{i\perp}$ and $\Delta T_{i\parallel}$ as a function of rf power as solid and dashed curves, respectively. The $T_{i\perp}$ - $T_{i\parallel}$ differential increases with power, since the higher temperature means the lower collisional coupling. This picture appears to be consistent with the experimental observation. In these ion-power-balance calculations, the Ohmic-level ion-energy transport coefficient [$\chi_i \approx 3\chi_i(\text{neoclassical})$] has been used.

An ion-heating process at $\frac{3}{2} \Omega_H$ has been observed in the particle-simulation investigation of IBW heating.⁹ This nonlinear process due to a type of stochastic acceleration at $\frac{3}{2} \Omega_H$ can directly heat the bulk ion distribution at relatively low power threshold ($\geq 15 \text{ kW}$ for the present experimental condition). This bulk-heating picture agrees with the experimentally observed, nearly Maxwellian, perpendicular velocity distribution [Fig. 2(c)]. Also recently, a possibility of the nonlinear Landau damping¹⁰ at $\frac{3}{2} \Omega_H$ has been pointed out showing that this process can occur at low power level.¹¹ This nonlinear process also heats bulk ions, since $\omega/k_{\perp} \approx V_{ii}$. Because of its wider effective interaction width ($\geq 1 \text{ cm}$) as opposed to the conventional cyclotron-harmonic damping ($\leq 1 \text{ cm}$), this process can absorb the wave completely before it reaches the harmonic absorption layer.¹¹ These theoretical pictures appear to be consistent with the experimental observation. We should note that, in this experiment, we have not observed significant electron heating, $\Delta T_e \leq 100 \text{ eV}$. This is not surprising, since with the present single-loop (unphased) antenna, very little direct electron heating is expected.

In conclusion, efficient bulk-hydrogen-ion heating by the externally launched ion-Bernstein wave has been observed in the JIPPT-II-U tokamak plasma. The heating efficiency is relatively insensitive to the minority-ion concentration; however, it is strongly optimized when the resonance layer is placed near the plasma axis. The hydrogen-ion temperature exhibits an increasing anisotropic behavior, $T_{i\perp} > T_{i\parallel}$, as the rf power is raised. The observations are generally consistent with presence of a direct hydrogen-heating process at the $\frac{3}{2} \Omega_H$ layer. This absorption mechanism

may be attractive, since it can be utilized to heat directly the bulk distribution of the majority fusion ions for better thermalization and confinement. It is therefore important to understand fully this $\frac{3}{2}\Omega_H$ heating mechanism for better control and extrapolation toward future heating experiments.

The present experiment was conducted as a Nagoya-Princeton collaboration project under the U.S.-Japan exchange program. The authors wish to express thanks to M. Mugishima and H. Ishiguro for their assistance in the experiments, and to K. Matuura and Y. Hamada for their continuous encouragement. The support of the RFC-XX group is also greatly appreciated. One of the authors (M.O.) thanks T. H. Stix, K. L. Wong, and members of the Princeton ACT-I team for their contributions in creating scientific bases leading to the present experiment. He also wishes to thank members of the PLT group for useful information and suggestions.

(a)Permanent Address: Princeton Plasma Physics Labora-

tory, Princeton, N.J. 08544.

¹M. Ono *et al.*, in *Heating in Toroidal Plasmas II*, edited by E. Cannobbio *et al.* (Pergamon, New York, 1981), Vol. 1, p. 593.

²M. Ono, G. A. Wurden, and K. L. Wong, Phys. Rev. Lett. **52**, 37 (1984).

³T. Amano *et al.*, in *Proceedings of the Ninth International Conference on Plasma Physics and Controlled Nuclear Fusion Research, Baltimore, 1982* (IAEA, Vienna, 1983).

⁴T. Watari *et al.*, Phys. Fluids **21**, 2076 (1978); T. Watari *et al.*, Nucl. Fusion **22**, 1359 (1983).

⁵F. Skiff, Ph.D. thesis, Princeton University, 1984 (unpublished).

⁶M. Ono, F. Skiff, and K. L. Wong, Bull. Am. Phys. Soc. **28**, 1126 (1983).

⁷M. Ono, K. L. Wong, and G. A. Wurden, Phys. Fluids **26**, 298 (1983).

⁸C. Singer *et al.*, Princeton Plasma Physics Laboratory Report No. PPPL-2073, 1984 (unpublished).

⁹H. Abe *et al.*, Phys. Rev. Lett. **53**, 1153 (1984).

¹⁰M. N. Rosenbluth *et al.*, Ann. Phys. (N.Y.) **55**, 248 (1969).

¹¹M. Porkolab, Phys. Rev. Lett. **54**, 434 (1985).